ENHANCED HEAT TRANSFER IN TUBES-IN-SHELL HEAT EXCHANGER FOR SYNGAS COOLING: A COMPARISON BETWEEN CONVENTIONAL AND PERFORATED TWISTED TAPE INSERTS

Nicolò Morselli[1], Filippo Ottani[1], Massimiliano Parenti[1], Paolo Tartarini[1]

[1] BEELab (Bio energy efficiency laboratory), Department of Engineering "Enzo Ferrari", University of Modena and Reggio Emilia, Via Vivarelli 10/1 – 41125 Modena, Italy.

ABSTRACT: In this work, twisted tape inserts were applied to a tube-in-shell heat exchanger for syngas cooling. A comparison between plain tube, standard full twisted tape and perforated twisted tape was carried out by measuring the thermal-hydraulic performance and the heat dissipated. Results shown a considerable increase of heat transfer using twisted tapes for syngas cooling and perforated twisted tapes performed better than full twisted tapes, reaching a thermal-hydraulic efficiency of 1.24 and increasing the Nu number up to 47% respect of the plain tube. Perforated twisted tapes confirmed the literature results even applied to syngas cooling and are of great interest as heat transfer enhancers to reduce the heat exchanger dimensions, key parameter for micro-scale gasification power plants.

Keywords: twisted tapes, heat transfer, gasification, syngas, biomass

1 INTRODUCTION

Twisted tapes are widely used in wood boilers heat exchangers to enhance the heat transfer between flue gas and water by reducing both the boundary layer and the convection resistance between the two fluids [1,2]. This study dealt with the experimental investigation of two different type of twisted tapes applied to a tubes in shell heat exchanger of a biomass gasification power plant for energy production.
In particular, the biomass power plant used in this work is a PP30 gasifier by ALL Power Labs [33], capable of 20 kW of electrical power output and 40 kW of thermal power through the use of the combined heat and power (CHP) module.
In this work, the original gas cooling device was replaced with a custom one which consists of a tubes in shell heat exchanger with 7 tubes, 37 mm inner diameter, 1.5 m long [3]. The syngas flows into the tubes and the cooling water in the shell.
Since the filtration stage downstream the heat exchanger is composed of a series of cloth filter, the temperature range of the syngas must be lowered between 60 °C and 150 °C in order to, respectively, avoid the water condensation and keep the fabric of the filter bags under the maximum working temperature [4-6]. To stay within this temperature range, the engine coolant was used as cooling water of the heat exchanger.
A comparison between the two sets of tapes was carried out by evaluating the HTC, the pressure loss and the total amount of thermal power transferred from the syngas to the coolant.

2 MATERIAL AND METHODS

2.1 Gasification facility

The PP30 (Figure 1) can be subdivided into different parts according to their function:

- the gas making stage ( ) that converts the woody biomass into fuel gas (syngas);
- the gas conditioning system that consists of a heat exchanger ( ) to cool down the gas and a filtering stage ( ) to reduce the amount of pollutants such as soot and tars [6,7, 8, 9];
- the internal combustion engine ( ), fueled by the syngas, that generates the electrical and thermal power output.

Figure 1. All Power Labs PP30 CHP [7].

In has been demonstrated in previous works that the PP30 gasifier can be fueled with wood chips [10, 34], agro industrial waste such as chipped vine prunings [11], corn cobs [12], corn stover [13, 14, 15], wood residues from river maintenance [16, 17], solid residues from vegetable oil production [18], solid residues from cotton crops [19] or municipal green waste [20].
In the following tests, the PP30 was fed with vine pruning pellets with an HHV of 19.3 MJ kg^{-1} [21] calculated according to [22] in order to have a stable and repeatable material.

2.2 Boundaries of the gas cooling

In every woody biomass gasification facility for CHP purpose, it is necessary to cool down the producer gas in order to make it suitable for the components downstream the gasification stage. In the PP30 three main components play a crucial role in defining the operation temperature of the system:

- IC engine: the engine has a compression ratio of 12.5:1 [23] and intake maximum temperature is in limited by the increasing risk of knocking with the increasing mixture temperature. Moreover, to increase the volumetric efficiency of the engine (when naturally-aspired), it's important to cool down as much as possible the mixture intake temperature [24, 25, 26].

- Producer gas filtration stage: the PP30 is provided with a multiple cloth-bag filtration stage which have a maximum working temperature of 150°C.
- On the other hand, cooling down the syngas under its dew point (50÷60 °C [4]) causes the condensation of water and tars that need to be immediately removed from the system avoiding the sticking or failure of mechanical components (e.g. engine intake valves, throttle plate, …). Since the PP30 is designed to run dry, the heat exchanger needs to be designed to cool down the gas while maintaining its temperature above 60°C.

Eventually, an HX for biomass gasification purposes needs also to deal with a relevant amount of PM (1÷5 g Nm^{-3}) that is carried in the gas stream and tends to foul the device, decreasing its effectiveness.

2.3 Test rig description

The facility used to test the two different sets of TT is part of a multiple tubes in shell HX that replaces the original heat exchanger from APL which cannot be fit with TT inserts.
The gas cooler, as a whole, is represented in Figure 2a and described more in detail in [3]. The device, as designed, is affected of a severe non-homogeneity in the distribution of the producer gas between the different tubes, since, the gas-flow, is higher in the central one than the others [3].
For this reason, to carry out the comparison between regular and perforated TT, the 6 peripherical tubes were plugged and only the central tube was used and fit with TT to test.
The so reduced HX consists of a single SS tube 37 mm ID, 1.5 mm thick and 1500 mm long (Figure 2b).

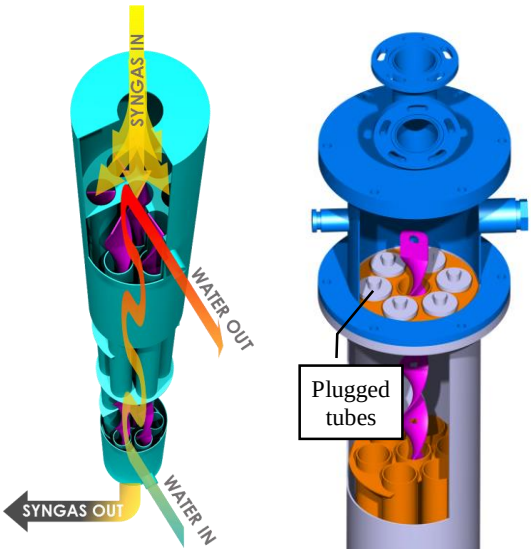

Figure 2. Full tubes-in-shell HX (a) and the reduced single-tube HX used for the tests (b).

To cool down the gas, maintaining its temperature above the dew point, the engine cooling system was used. Through a thermostat device, the coolant was kept at temperatures above 70 °C avoiding cold spots in the HX.
In normal engine operation, the engine is connected to the cooling system and it provides the heat necessary to warm up the water from ambient temperature to operating temperature.

Both the gas and the coolant side were provided with T-type and K-type thermocouples to measure the inlet and outlet temperatures of the fluids. A calibrated orifice meter, provided with a K-type thermocouple, was used to measure the gas flow.
The coolant motion is provided by an electrical water centrifugal pump and, while the water flowrate is fixed, the gas flow can be adjusted by modifying the electrical power generated by the engine.

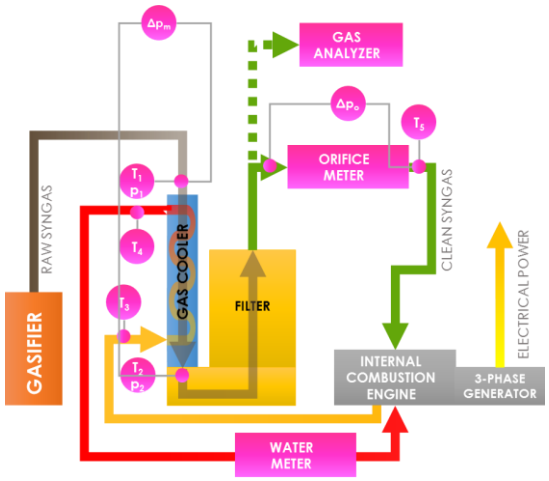

Figure 3. Test rig schematics

2.3 Twisted tapes description

The two sets twisted tapes have the length of 1.6 m and the width of 33 mm in order to guarantee enough clearance between the tape and the tube, even in presence of soot deposition. The twist ratio of the tapes was set to 200 mm (calculated on 180°) and the second set of tapes has, in addition, equispaced square holes (Figure 4).

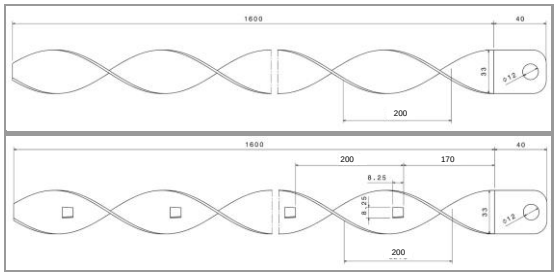

Figure 4. Standard and perforated TT used in the tests.

2.4 Data reduction

The producer gas mass flow rate was determined by measuring the pressure drop at the calibrated orifice and calculated by using the following formula [27]:

$$\dot{m}_g = C_d A_o \left[\frac{2\rho(\Delta p)_o}{1-\beta^4}\right]^{0.5} \quad (1)$$

The gas velocity can thus be calculated according to:

$$v_g = \frac{\dot{m}_g}{\rho_g \cdot A_t} \quad (2)$$

To understand the flow regime, the Reynolds number is calculated:

$$Re = \frac{v_g \cdot D_t \cdot \rho_g}{\mu_g} \tag{3}$$

The measure of the pressure drop across the tube, leads to the estimation of the friction factor according to the Darcy equation [27]:

$$f_D = \frac{2 \cdot D_t \cdot \Delta p_t}{\rho_g \cdot L \cdot v_g^2} \tag{4}$$

This coefficient is crucial in determining the friction losses of the selected shape of TT against plain tube.
Since it was not possible to instrument the tube surface of the HX to measure the mean tube wall temperature, the calculation of the *Nu* number could not go through the intermediate calculation of h_g and an alternative approach was used and explained in the following paragraph.

2.5 Approximate procedure for the estimation of the gas-side Nusselt number

The HX power output and the overall heat transfer coefficient were calculated by [28]:

$$\dot{Q}_g = \dot{m}_g \cdot c_{p,g} \cdot (T_{g,IN} - T_{g,OUT}) \tag{5}$$

$$HTC_g = \frac{\dot{Q}_g}{A_{HX}\, \Delta T_{LM}} \tag{6}$$

Where:

$$\Delta T_{LM} = \frac{\Delta T_1 - \Delta T_2}{\log(\frac{\Delta T_1}{\Delta T_2})} \tag{7}$$

And:

$$\Delta T_1 = T_{g,IN} - T_{w,OUT}$$
$$\Delta T_2 = T_{g,OUT} - T_{w,IN} \tag{8}$$

By using the correlation between HTC and thermal resistance, the internal convective heat transfer coefficient could be found as follows:

$$R_{TOT} = \frac{1}{HTC \cdot A_{HX}} \tag{9}$$

$$R_{TOT} = R_{conv,w} + R_{cond,m} + R_{conv,g} \tag{10}$$

Where:

$$R_{conv,w} = \frac{1}{A_{HX} \cdot h_w} \tag{11}$$

$$R_{cond,m} = \frac{\ln\left(\frac{D_e}{D_i}\right)}{2 \cdot \pi \cdot k \cdot L} \tag{12}$$

$$R_{conv,g} = \frac{1}{A_{HX} \cdot h_g} \tag{13}$$

Since, in this case, the convective heat transfer coefficient for water systems is far higher than for the gas ones, this estimation can lead to a more robust results than the direct estimation of h_g. Hence, in this method, h_w was estimated by the following equation [29]:

$$h_w = h'_w\, F_B\, F_I\, F_W \tag{14}$$

Where F_x are correction factors for tubes in shell heat exchanger and h'_w is calculated according to the following empirical correlation [29]:

$$h'_w = 0.32 \frac{\lambda_w}{D_t} \left(\frac{G_c D_t}{\mu}\right)^{0.61} \left(\frac{c_p \mu}{\lambda_w}\right)^{\frac{1}{3}} \left(\frac{\mu}{\mu_{wall}}\right)^{0.14} \tag{15}$$

The convective heat transfer coefficient on the gas side could be calculated as follows:

$$h_g = \frac{1}{A_{HX} \cdot (R_{TOT} - R_{conv,w} - R_{cond,m})} \tag{16}$$

And, hence, the Nusselt number according to:

$$Nu_{TT} = \frac{h_g \cdot D_t}{\lambda_g} \tag{17}$$

The Nusselt number is needed to calculate the thermal-hydraulic performance of the different configurations: a critical parameter that helps to compare the enhanced performance of the heat exchangers with respect to plain tube heat exchanger.

$$\eta_p = \frac{\left(\frac{Nu_{TT}}{Nu_{PT}}\right)}{\left(\frac{f_{TT}}{f_{PT}}\right)^{\frac{1}{3}}} \tag{18}$$

2.4 Validation of experimental results

Experimental results for plain tube were validated with Gnielinski's [30] equation (Eq. 19) for the Nu_{pt} calculation and Petukhov's equation for the friction factor f_{pt} (Eq. 20).

$$Nu_{PT,Gn} = \frac{\frac{f_{PT,Pe}}{8} \cdot (Re_n - 1000)\mathrm{Pr}^*}{1 + 12.7\left(\frac{f_{PT,Pe}}{8}\right)^{0.5} ((\mathrm{Pr}^*)^{\frac{2}{3}} - 1)} \quad 10^3 < Re < 5 \cdot 10^6 \tag{19}$$

$$f_{PT,Pe} = (0.79 \ln(Re_n^{-0.25}) - 1.64)^{-2} \quad 3000 < Re < 5 \cdot 10^6 \tag{20}$$

Where, to take into account the roughness of the tube, the modified Prandtl number is given by [31]:

$$Pr^* = \frac{f_{PT,exp}}{f_{PT,Pe}} \cdot Pr \qquad 0.5 < Pr < 3.0 \tag{21}$$

The comparison between empirical and experimental results, for plain tubes, is necessary to confirm the accuracy of the experimentally collected data.

2.6 Tests methodology

In this work, three configurations were tested: plain tube (PT_exp), plain tube + standard full twisted tape (TT_STD_exp) and plain tube + perforated twisted tape (TT_perf_exp). The results, calculated according to the previous paragraphs, are reported in the next chapter following the above nomenclature.
Before each test, the heat exchanger tube was cleaned from carbon and tars deposits in order to have the same wall conditions for each configuration.
Each configuration was tested in several conditions of flowrate in order to investigate the trend of the heat exchange capability. The flowrate was modified by increasing or decreasing the electrical power output of the gas engine connected to the gasifier. The higher the power drawn from the engine, the higher the syngas flowrate. The maximum flowrate is limited by the maximum temperature of the filter bags, installed in the filtration stage, set to 150°C.

3 RESULTS

3.1 Validation of experimental results

In Figure 5 a comparison between the experimental friction factor and the one calculated according to Petukhov's correlation is presented. The discrepancy between the results suggests that the test tube is far from smooth conditions and, for this reason, the proposed rough tube approach (Equations 19-21) is justified.

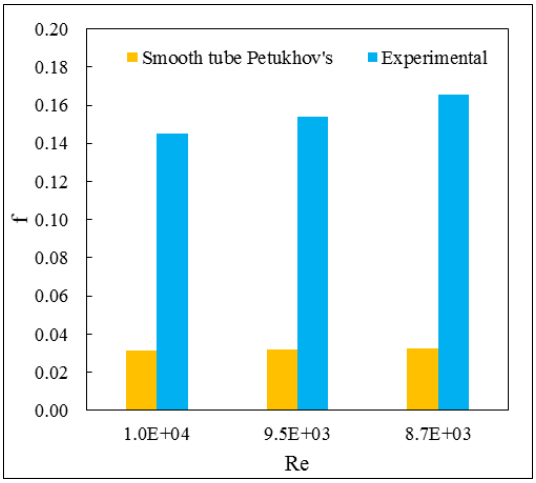

Figure 5. friction factor comparison for smooth tube.

To confirm the rough-tube approach, in the Figure 6 the Nusselt comparison between experimental and the modified Gnielinski's is reported. The difference between theoretical and experimental model is less than 2%.

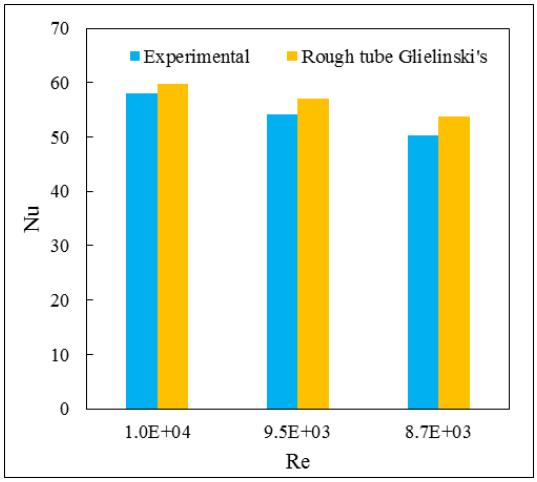

Figure 6. Nusselt comparison with the modified rough-tube correlation.

3.2 Heat transfer comparison using twisted tapes

Nusselt and friction factors were calculated according to the previous equations and are plotted versus the Reynolds number in Figure 7 and Figure 8.

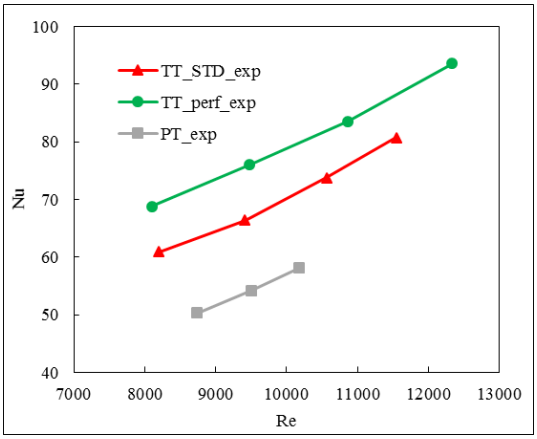

Figure 7. Variation of Nusselt vs Reynolds of the different configurations.

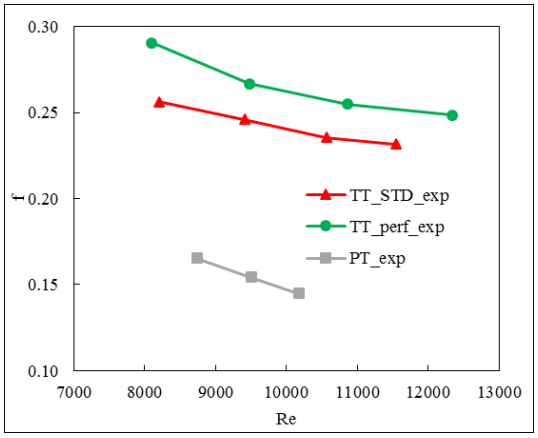

Figure 8. Variation of friction factor vs Reynolds of the different configurations.

Another comparison is proposed from Figure 9 to Figure 11 where the heat dissipated, the overall heat transfer coefficient and the gas outlet temperature from the heat exchanger are reported according to the different tested configurations.

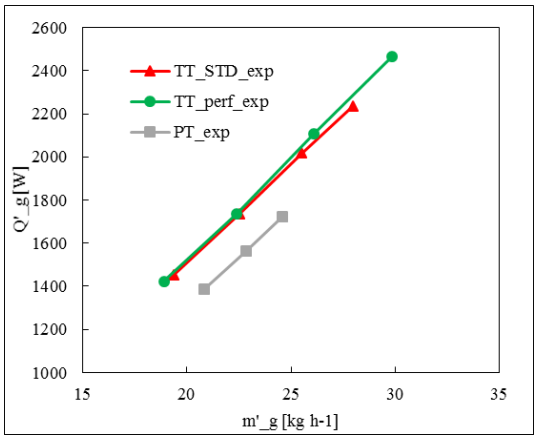

Figure 9. Thermal power gained from the heat exchanger vs the gas mass flowrate: comparison between the different configurations.

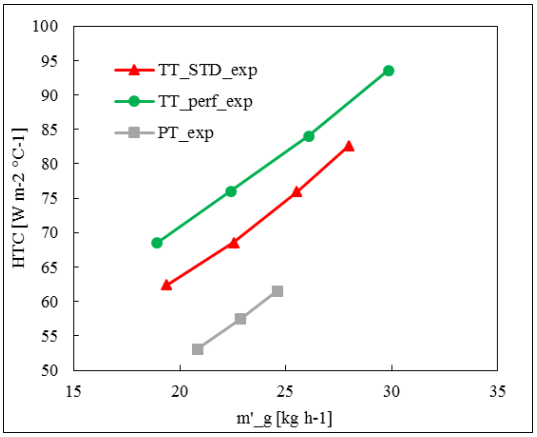

Figure 10. Overall heat transfer coefficient at different gas mass flowrate: comparison between the different configurations.

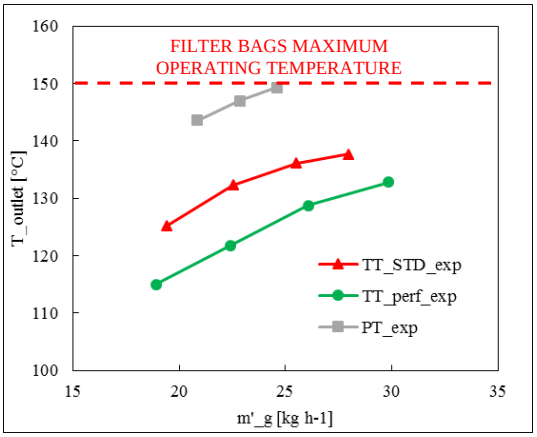

Figure 11. Gas outlet temperature from the heat exchanger: comparison between the different configurations.

3.3 Thermal-hydraulic performance factor

The thermal-hydraulic performance factor is reported in Figure 12 and referred to experimental measurement of the plain tube.

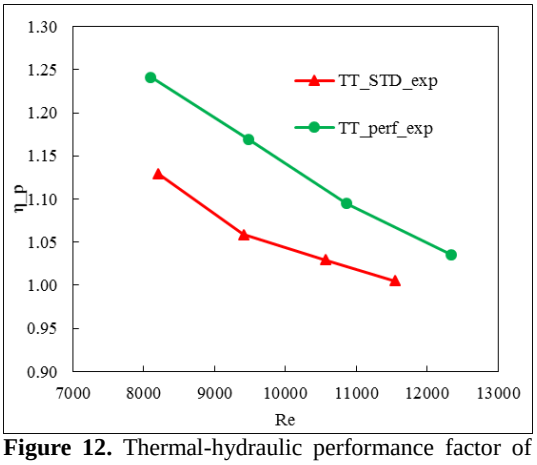

Figure 12. Thermal-hydraulic performance factor of the full and perforated twisted-tapes.

4 CONCLUSIONS

In this work, perforated and standard full twisted tapes were applied to a gas/water heat exchanger used as a gas cooler in a small gasification power plant.
Plain tube heat transfer capacity was tested in order to verify the test rig. The Prandtl number in the Gnielinski's correlation for smooth tube was modified in order consider the roughness of the tube. The modified Gnielinski's according to [31] guarantees a discrepancy lower than 7% between experimental and empirical correlation and can be considered accurate.
Comparing perforated and full twisted tape with the plain tube, results shown an increase of the Nusselt number up to 29% for full TT and up to 47% for perforated TT.
On the other hand, the use of twisted tapes increased the friction factor of the 85% for full TT and 118% for perforated TT.
In order to evaluate the global cooling performance of the tested TTs, the thermal-hydraulic coefficient was calculated for each configuration, showing results up to 1.13 for full TT and up to 1.24 for perforated TT and declaring the convenience of their use, confirming the literature results [1, 2, 32].
Twisted tapes applied to syngas cooling shown a clear increase of the heat transfer which results in lower gas temperature at the heat exchanger (Figure 11). This result led to the possibility of more compact heat exchanger, suitable for small/micro-scale gasification power plant.
Moreover, also in this case-study, stands out the possibility to implement a cleaning mechanism of the heat exchanger by means of the sliding up and down of the twisted tapes.

5 REFERENCES

[1] Bipin K, Gaurav P S, Manoj K, Anil K P 2018 A review of heat transfer and fluid flow mechanism in heat exchanger tube with inserts (Chemical Engineering & Processing: Process Intensification 123) pp 126–137.

[2] Eiamsa-ard S, Yongsiri K, Nanan K, Thianpong C 2012 Heat transfer augmentation by helically twisted tapes as swirl and turbulence promoters (Chemical Engineering Process 60) pp 42–48.

[3] Morselli N., Puglia M., Mason J., Parenti M., Ottani F., Tartarini P., "Experimental and modeling evaluation of possible solutions for compact design of producer gas heat exchangers", 2019, Journal of Physics: Conference Series. Article in press.

[4] SERI Generator Gas: The Swedish Experience from 1939-1945, Di Ingenjörsvetenskapsakademien (Sweden). Solar Energy Research Institute, United States. Dept. of Energy, Golden, Colorado, 1979.

[5] Reed T. B., Das A., Handbook of Biomass Downdraft Gasifier Engine Systems. The biomass energy foundation press, 1988.

[6] Morselli N., Puglia M., Parenti M., Tartarini P., "Use of Fabric Filters for syngas dry filtration in small-scale gasification power systems", 2019, AIP Conference Proceedings 2191, 020117 DOI: 10.1063/1.5138850

[7] Pedrazzi S., Allesina G., Sebastianelli L., Puglia M., Morselli N., Tartarini P., "Chemically enhanced char for syngas filtering purposes" European Biomass Conference and Exhibition Proceedings, 2018 (26thEUBCE), pp. 694-698.

[8] Quinlan B., Kaufmann B., Allesina G., Pedrazzi S., Hasty J., Puglia M., Morselli N., Tartarini P., "The use of on-line colorimetry for tar content evaluation in gasification systems" International Journal of Heat and Technology, 35 (Special Issue 1), pp. S145-S151.

[9] Morselli N., Allesina G., Pedrazzi S., Puglia M., Mason J., Lemberger A., Tartarini P., "Use of gasification char for hot gas filtration in micro-scale power plants" European Biomass Conference and Exhibition Proceedings, 2018 (26thEUBCE), pp. 465-469.

[10] Pedrazzi S, Allesina G and Tartarini P. 2012 Aige conference: A kinetic model for a stratified downdraft gasifier (International Journal of Heat and Technology, vol. 30, no. 1) pp. 41-44

[11] Allesina G, Pedrazzi S, Puglia M, Morselli N, Allegretti F, Tartarini P 2018 Gasification and Wine Industry: Report on the Use Vine Pruning as Fuel in Small-scale Gasifiers (European Biomass Conference and Exhibition Proceedings (26thEUBCE)) pp. 722-725

[12] Allesina, G., Pedrazzi, S., Sgarbi, F., Pompeo, E., Roberti, C., Cristiano, V., Tartarini, P 2015 Approaching sustainable development through energy management, the case of Fongo Tongo, Cameroon (International Journal of Energy and Environmental Engineering, vol. 6, no. 2) pp. 121-127

[13] S. Pedrazzi, G. Allesina, M. Puglia, L. Guidetti, P. Tartarini, Increased maize power production through an integrated biomas-gasification-SOFC power system, The Proceedings of the International Conference on Power Engineering (ICOPE) 2015, DOI: 10.1299/jsmeicope.2015.12._ICOPE-15-_2

[14] Allesina G, Pedrazzi S, Montermini L, Giorgini L, Bortolani G and Tartarini P 2014 Porous filtering media comparison through wet and dry sampling of fixed bed gasification (J. Phys. Conf. Series, vol. 547)

[15] Allesina G, Pedrazzi S, Guidetti L and Tartarini P 2015 Modeling of coupling gasification and anaerobic digestion processes for maize bioenergy conversion (Biomass and Bioenergy, vol. 81) pp. 444-451

[16] Pedrazzi S, Allesina G, Morselli N, Puglia M, Barbieri L, Lancellotti I, Ceotto E, Giorgini L, Malcevschi A, Pederzini C and Tartarini P, 2017 The energetic recover of biomass from river maintenance: the REBAF project (European Biomass Conference and Exhibition Proceedings, 25thEUBCE) pp. 52-57

[17] Allesina G, Pedrazzi S, Ginaldi F, Cappelli G A, Puglia M, Morselli N and Tartarini P 2018 Energy production and carbon sequestration in wet areas of Emilia Romagna region, the role of Arundo Donax (Advances in Modelling and Analysis A, 55 (3)) pp. 108-113

[18] Allesina G, Pedrazzi S, Tebianian S and Tartarini P 2014 Biodiesel and electrical power production through vegetable oil extraction and byproducts gasification: Modeling of the system (Bioresource Technology, vol. 170) pp. 278-285

[19] Allesina G, Pedrazzi S, Allegretti F, Morselli N, Puglia M, Santunione G and Tartarini P 2018 Gasification of cotton crop residues for combined power and biochar production in Mozambique (Applied Thermal Engineering, vol. 139) pp. 387-394

[20] Pedrazzi S, Santunione G, Minarelli A, Allesina G 2019 Energy and biochar co-production from municipal green waste gasification: A model applied to a landfill in the north of Italy (Energy Conversion and Management, vol. 187) pp. 274-282

[21] Pedrazzi S, Morselli N, Puglia M, Tartarini P, Energy and emissions analysis of hemp hurd and vine pruning derived pellets used as fuel in a commercial stove for residential heating. Italian Journal of Engineering Science. Article in press.

[22] Puglia M., Pedrazzi S., Allesina G., Morselli N., Tartarini P., "Carbonization of residual biomass from river maintenance using waste heat from gasification power plants" European Biomass Conference and Exhibition Proceedings, 2018 (26thEUBCE), pp. 1127-1130.

[23] Mason, J., Kaufmann, B., Tartarini, P., Puglia, M., Morselli, N., Veratti, G., Bigi, A, Compression Ratios Comparisons between Engines Operating with Producer Gas, European Biomass Conference and Exhibition Proceedings, Volume 2019, Issue 27thEUBCE, 2019, pp 1927 – 1931, DOI: 10.5071/27thEUBCE2019-IBV.1.8

[24] Heywood J 1988 Internal Combustion Engine Fundamentals, McGraw-Hill

[25] G. Allesina, S. Pedrazzi, L. Arru, M. Altunöz, M. Puglia, P. Tartarini, Uses of a water-algae-photo-bio-scrubber for syngas upgrading and purification, European Biomass Conference and Exhibition Proceedings, Volume 2016, Issue 24thEUBCE, 2016, Pag. 944-947, DOI: 10.5071/24thEUBCE2016-2CV.3.62

[26] Simone Pedrazzi, Giulio Allesina, Nicolò Morselli, Marco Puglia, Chiara Leonardi, Carlo Alberto Rinaldini, Tommaso Savioli, Enrico Mattarelli, Loris Giorgini, Paolo Tartarini. "Modified diesel engine fueled by syngas: modeling and experimental validation." 24th European Biomass Conference & Exhibition (EUBCE 2016).

[27] Amar Raj Singh Suri, Anil Kumar, Rajesh Maithani. Heat transfer enhancement of heat exchanger tube with multiple square perforated twisted tape inserts: Experimental investigation and correlation development. Chemical Engineering and Processing 116 (2017) 76–96

[28] Cengel Y. A., Introduction to thermodynamics and heat transfer. McGraw-Hill, 1997.

[29] Andreini P, 2019 Manuale dell'ingegnere meccanico. (Hoepli) pp. 1661-1671

[30] Gnielinski V, On heat transfer in tubes. International Journal of Heat and Mass Transfer 63 (2013) 134–140

[31] Numrich R., 1990, Heat Transfer in Rough Tubes.Fachgruppe Verfahrenstechnik, Universitiit-GH-Paderborn, Posfach 1621, 4790 Paderborn.

[32] Kumar A, Kumar M, Chamoli S, Comparative study for thermal-hydraulic performance of circular tube with inserts, 2014, Alexandria Engineering Journal. Short communication.

[33] ALL Power Labs, website: www.allpowerlabs.com

[34] Allesina G., Pedrazzi S., Rinaldini C. A., Morselli N., Savioli T., Mattarelli E., Tartarini P., "Experimental-analytical evaluation of sustainable syngas-biodiesel CHP systems based on oleaginous crops rotation." Proceedings of the International Conference on Power Engineering-15 (ICOPE-15), code 118770. November 30- December 4, 2015,

Yokohama, Japan DOI: 10.1299/jsmeicope.2015.12._ICOPE-15-_1

6 NOMENCLATURE

HX	Heat exchanger
$\dot{m}_g$	Gas mass flowrate, kg s^{-1}
C_d	Coefficient of discharge
A_o	Orifice surface, m
ρ	Gas density, kg m^{-3}
Δp_o	Pressure difference generated by the orifice, Pa
β	Ratio between small and large diameter of the orifice
v_g	Gas velocity, m s^{-1}
A_t	Tube section surface, m
Re	Reynolds number
D_t	Tube inner diameter, m
μ	Gas dynamic viscosity, kg m^{-1} s^{-1}
f_D	Darcy friction factor
Δp_t	Head loss across the tube, Pa
L	Tube length, m
η_p	Thermal and hydraulic performance
Nu	Nusselt number
Pr	Prandtl number
$\dot{Q}_g$	Heat exchanger power output, W
$c_{p,g}$	Specific heat capacity of the gas, J kg^{-1} $°C^{-1}$
T_g	Gas temperature, °C
T_w	Water temperature, °C
HTC_g	Overall heat transfer coefficient, W m^{-2} $°C^{-1}$
A_{HX}	Heat transfer surface of the heat exchanger, m^2
ΔT_{LM}	Logarithmic mean temperature difference, °C
R	Thermal resistance, °C W^{-1}
h_g	Gas convective heat transfer coefficient, W m^{-2} $°C^{-1}$
h_w	Water convective heat transfer coefficient, W m^{-2} $°C^{-1}$
G_c	Water specific transverse flowrate, kg s^{-1} m^{-2}
Subscripts	
TT	Tube equipped with twisted tape
PT	Plain tube (without twisted tape)
IN	Referred to gas or water inlet
OUT	Referred to gas or water outlet
m	Referred to the metal of the tube
conv	Convective
cond	Conductive
Gn	Gnielinski
DB	Dittus-Boelter
Bl	Blasius
Pe	Petukhov

7 ACKNOWLEDGEMENTS

A sincere thanks to the *All Power Labs Inc.* company for having made available to our research the Power Pallet 30 biomass power plant and also thanks to *La Golena* winery farm in Modena (IT) for hosting the facility.

8 LOGO SPACE

Iniziativa realizzata nell'ambito del Programma regionale di sviluppo rurale 2014-2020 – Tipo di operazione 16.1.01 – Gruppi operativi del partenariato europeo per l'innovazione: "produttività e sostenibilità dell'agricoltura"
Focus Area 5C – Progetto "Valorizzazione dei sottoprodotti della filiera vitivinicola - Val.So.Vitis

Programma di Sviluppo Rurale dell'Emilia-Romagna 2014-2020
UNIONE EUROPEA
RegioneEmilia-Romagna
L'Europa investe nelle zone rurali

LINK PORTALE CRPV:
https://progetti.crpv.it/Home/ProjectDetail/26